

Supplement to “Evaluating the performance of pyrogenic and biogenic emission inventories against one decade of space-based formaldehyde columns”

T. Stavrakou¹, J.-F. Müller¹, I. De Smedt¹, M. Van Roozendael¹, G. R. van der Werf², L. Giglio³, and A. Guenther⁴

¹Belgian Institute for Space Aeronomy, Avenue Circulaire 3, 1180, Brussels, Belgium

²Faculty of Earth and Life Sciences, Vrije Universiteit Amsterdam, De Boelelaan 1085, 1081 HV Amsterdam, The Netherlands

³Science Systems and Applications, Inc. NASA Goddard Space Flight Center, Greenbelt, Maryland 20771, USA

⁴National Center for Atmospheric Research, Boulder, CO 80303, U.S.A.

The present supplement is composed of three parts. In the first part we describe the pyrogenic and biogenic emission databases which are used in this study. The second part presents the chemical mechanism of the NMVOCs used in IMAGESv2 model. The chemical species and the kinetic reactions are presented in Tables 2 and 3, respectively. The photodissociations are summarized in Table 4. The last part contains auxiliary material of the Section 4 of the manuscript.

Part A

Pyrogenic Emission Inventories

The Global Fire Emissions Database (GFED) version 1 (van der Werf et al., 2004) and version 2 (van der Werf et al. (2006) cover the period from 1997 to 2006. They combine information on burned area for selected regions (Giglio et al., 2006) with fire hot spot data (Giglio et al., 2003; Justice et al., 2002), and biogeochemical modelling to estimate carbon emissions (van der Werf et al., 2003). Emission factors provided by Andreae and Merlet (2001) with updates from M.O. Andreae (personal communication, 2007) have been used to derive trace gas emissions from the carbon emissions.

The GFEDv1, released in 2004, is based on a single relation between burned area from 16 MODIS “tiles”, each covering an area of 10×10 degrees, and TRMM-VIRS fire hot spots. This relation is dependent on the tree cover fraction; in general, one hot spot represents more burned area in grassland than in forests due to the faster spread rate in grassland, and thus the smaller probability of detection (van der Werf et al., 2003).

Burned area reprocessing and refinements to the biogeochemical model, resulted in a new version of GFED, released in 2006 (GFEDv2). The main differences with the first version stem from the use of MODIS hot spots, a much larger

number of burned area tiles that are processed (446), a regional fire hot spot to burned area relation (Giglio et al., 2006), the inclusion of combustion of belowground carbon, and the use of fire persistence to increase combustion completeness due to multiple ignitions in deforestation regions. The large number of tiles allows for a regional fire hot spot/burned area model to account for regional variations in the use of fire. The model uses also herbaceous vegetation cover, the mean size of monthly cumulative fire-pixel clusters size, and regression trees in order to derive the fire hot spot/burned area relation (Giglio et al., 2006). More specifically, in GFEDv1 only above ground biomass can burn. However, especially in the boreal regions and Indonesia, below ground carbon also burns. Regionally this source may be more important than the combustion of above ground biomass. Another modification is based on fire persistence; in areas undergoing deforestation, fuels are often ignited multiple times to enhance the combustion completeness. This translates into several fire observations over a period of weeks to months within one location. Where this is observed, the combustion completeness is increased in GFEDv2.

Zonally and monthly averaged NMVOC emissions derived from the GFEDv1 and GFEDv2 databases are displayed in Fig.1, as well as their annual global estimate. The average global NMVOC emissions amount to 109 Tg/yr and 96 Tg/yr according to GFEDv1 and GFEDv2, respectively. In general, version 2 has lower overall emissions (due to lower burned area) but higher interannual variability (as this variability stems mostly from fires in deforestation regions and areas where belowground carbon burning is important), and the peak fire season is delayed by a month in the Southern Hemisphere (due to the use of MODIS fire spots instead of those derived from TRMM). The highest NMVOC emissions occur during the El Niño years 1997–1998, whereas the lowest values occur in 2000/2001 for the GFEDv2 and in 2006 for the GFEDv1 database.

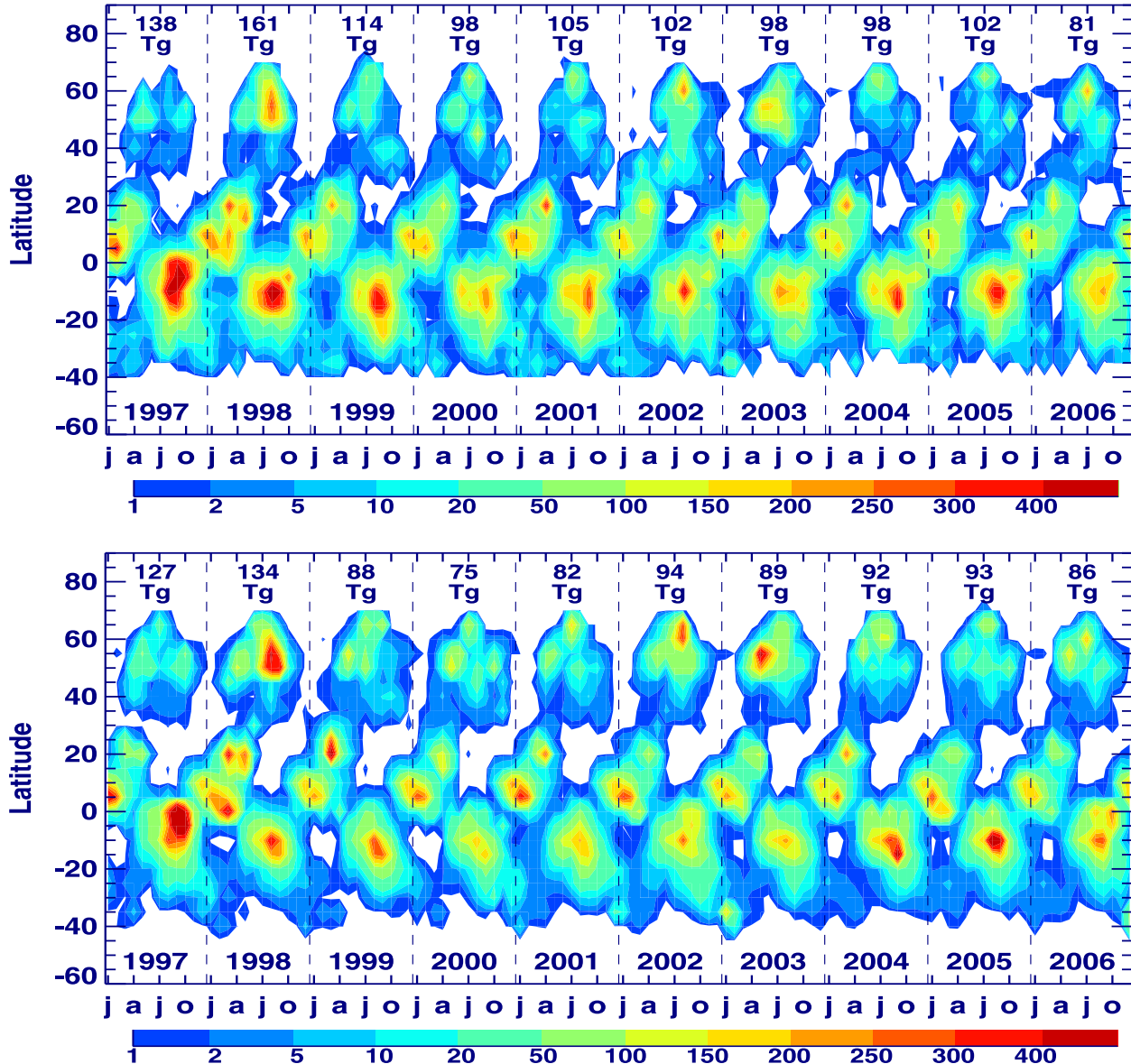


Fig. 1. Zonally and monthly averaged NMVOC emissions ($\mu\text{g}/\text{m}^2/\text{hour}$) calculated using the emission factors provided by Andreae and Merlet (2001) with updates from M.O. Andreae (personal communication, 2007) and the global biomass burnt estimate from the GFEDv1 (top figure) and GFEDv2 (bottom figure) database.

Biogenic Emission Inventories

Biogenic emissions of isoprene are calculated using the MEGAN model (Guenther et al., 2006) coupled with the MOHYCAN canopy environment model (Wallens, 2004; Müller et al., 2008). The emissions are calculated off-line at a high spatial ($0.5^\circ \times 0.5^\circ$) and temporal (hourly) resolution, and then regredded at the resolution of the IMAGESv2 model ($5^\circ \times 5^\circ$, daily). Monoterpene emissions are neglected. The isoprene emission rate E at a specific location and time is expressed as

$$E = 0.52 \cdot \epsilon \cdot \left(\sum_k (\gamma_P)_k \cdot (\gamma_T)_k \cdot (\text{LAI})_k \right) \cdot \gamma_{\text{age}} \cdot \gamma_{\text{SM}}, \quad (1)$$

where ϵ (mg/m²/h) represents the emission at standardized conditions defined in Guenther et al. (2006). The factor 0.52 is necessary to ensure that $E = \epsilon$ for these standard conditions. The response to the photosynthetic photon flux density (PPFD, $\mu\text{mol}/\text{m}^2/\text{s}$) and the leaf temperature is taken into account by γ_P and γ_T emission activity factors (Guenther et al., 2006), respectively. LAI is the leaf area index. The index k runs over the layers of the canopy model, which provides the incident PPFD and temperature of sun and shade leaves at each of the depths of the modelled canopy, and is driven by values at the canopy top of PPFD and near infrared radiation flux, relative humidity, air temperature, and windspeed (Müller et al., 2008). The factor γ_{age} , representing the dependence on the leaf growth state for deciduous canopies, is parameterized from LAI changes between current and previous time steps (Guenther et al., 2006). The factor γ_{SM} accounts for the emission response to soil moisture stress. The total emission for a given location is expressed as the sum of the emissions calculated for all the plant functional types present in the given model grid cell, for clear sky and cloudy conditions.

We drive MEGAN with ECMWF fields for the downward solar flux, the cloud cover fraction, as well as for the air temperature, dewpoint temperature, and windspeed directly above the canopy. Reanalysed ERA40 fields are used until 2001 and operational analyses are used beyond this date. Monthly mean LAI values derived from the MODIS satellite instrument (Zhang et al., 2004) from 2001 onwards are used, and a climatological mean over 2001-2006 is used before this date. The landcover is taken from Guenther et al. (2006). The soil moisture is provided by the ECMWF/ERA40 model analyses, and the soil moisture at the permanent wilting point is taken to the value used in the ECMWF model (0.171 m³/m³).

We determine the PPFD under clear sky conditions by using a radiative transfer model (Madronich and Flocke, 1998), and the ratio of the PPFD to the total solar radiation from the ISCCP dataset (Rossow et al. (1996), <http://isccp.giss.nasa.gov/>). Using the cloud cover fraction and the total solar radiation flux, the cloud optical

Table 1. Isoprene emission estimates by region from the GEIA database and from the MEGAN-ECMWF mean value over the 1997-2006 period. Numbers in parentheses refer to the minimum and maximum emission flux over the 10-year period.

Regions	GEIA	MEGAN-ECMWF
North America	51.8	44.4 (41.0-49.3)
eastern US	11.7	10.9 (9.3-12.8)
Europe	11.6	6.1 (5.5-6.8)
South America	203.4	127.2 (119.8-138.5)
Amazonia	130.1	83.2 (78.7-91.3)
Africa	148.9	96.4 (88.0-113.4)
Asia	119.1	88 (79.3-96.9)
Indonesia	36.9	35.5 (30.4-40.0)
Oceania	33.8	67 (60.4-73.0)
Globe	568	429 (394-478)

depth is determined, and thereby, the PPFD in cloudy conditions. The PPFD and near infrared fluxes for cloudy and non-cloudy skies are used as input in the canopy model. A thorough description of the emission inventory can be found in Müller et al. (2008) and the monthly averaged emissions (in mg isoprene/m²/hr) at a resolution of 0.5 degree are available in NetCDF format at the www.aeronome.be/tropo/models/mohycan.htm website.

The emissions are daily averaged and gridded onto the resolution of IMAGESv2. Globally, the MEGAN-ECMWF annual estimates are about 30% lower than the standard MEGAN estimate (Guenther et al., 2006). The difference is mainly due to the impact of the soil moisture stress factor which is found to decrease the global emission estimates by more than 20% (Müller et al., 2008). The GEIA database (Guenther et al., 1995) is used in this study as an alternative prior inventory. The differences between the GEIA and the MEGAN-ECMWF databases are mainly related to the emission algorithms used. The MEGAN model is based on an extensive compilation of field measurements, and includes the dependencies of the emission on the leaf age and on the soil moisture stress factor. In addition to this, the emissions of the MEGAN-based inventory account for the diurnal, daily, seasonal and year-to-year variability, while the GEIA inventory provides one emission field per month without accounting for the interannual variability due to the changing meteorology. A comparison between the isoprene flux estimates by region from GEIA and MEGAN-ECMWF are summarized in Table 1.

References

- Andreae, M. O. and P. Merlet: Emission of trace gases and aerosols from biomass burning, *Global Biogeochem. Cycles*, 15, 955–966, 2001.
- Giglio, L., J. D. Kendall, and R. Mack: A multi-year active fire dataset for the tropics derived from the TRMM VIRS, *Intern. J. of Remote Sensing*, 24 (22), 4505–4525, 2003.
- Giglio, L., G. R. van der Werf, J. T. Randerson, G. J. Collatz, and P. Kasibhatla: Global estimation of burned area using MODIS active fire observations, *Atmos. Chem. Phys.*, 6, 957–974, 2006.
- Guenther, A., C. N. Hewitt, D. Erickson, R. Fall, C. Geron, T. Graedel, P. Harley, L. Klinger, M. Lerdau, W. A. McKay, T. Pierce, B. Scholes, R. Steinbrecher, R. Tallamraju, J. Taylor, and P. Zimmerman: A global model of natural volatile organic compound emissions, *J. Geophys. Res.*, 100, 8873–8892, 1995.
- Guenther, A., T. Karl, P. Harley, C. Wiedinmyer, P. I. Palmer, and C. Geron: Estimates of the global terrestrial isoprene emissions using MEGAN (Model of Emissions of Gases and Aerosols from Nature), *Atmos. Chem. Phys.*, 6, 3181–3210, 2006.
- Justice, C. O., L. Giglio, S. Korontzi, J. Owens, J. T. Morisette, D. Roy, J. Descloitres, S. Alleaume, F. Petitcolin, and Y. Kaufman: The MODIS fire products, *Remote Sensing of Environment*, 83, (1-2), 244–262, 2002.
- Madronich, S. and S. Flocke: The role of solar radiation in atmospheric chemistry, in *Handbook of Environmental Chemistry*, edited by: Boule, P., Springer Verlag, Heidelberg, 1–26, 1998.
- M'uller, J.-F., T. Stavrakou, S. Wallens, I. De Smedt, M. Van Roozendael, M.. Potosnak, J. Rinne, B. Munger, A. Goldstein, and A. Guenther: Global isoprene emissions estimates using MEGAN, ECMWF analyses and a detailed canopy environment model, *Atmos. Chem. Phys.*, 8, 1329–1341, 2008.
- Rossow, W. B., A. W. Walker, D. E. Beuschel, and M. D. Roiter: International Satellite Cloud Climatology Project (ISCCP) Documentation of New Cloud Datasets, Report WMO/TD-No. 737, World Meteorological Organization, Geneva, 115 pp., 1996.
- van der Werf, G. R., J. T. Randerson, G. J. Collatz, and L. Giglio: Carbon emissions from fires in tropical and subtropical ecosystems, *Global Change Biology*, 9, 547–562, 2003.
- van der Werf, G. R., J. T. Randerson, G. J. Collatz, L. Giglio, P. S. Kasibhatla, A. F. Arellano, Jr., S. C. Olsen, and E. S. Kasischke: Continental scale partitioning of fire emissions during the 1997 to 2001 El Niño/La Niña period, *Science*, 303, 73–76, 2004.
- van der Werf G. R., J. T. Randerson, L. Giglio, G. J. Collatz, P. S. Kasibhatla, A. F. Arellano, Jr.: Interannual variability in global biomass burning emissions from 1997 to 2004, *Atmos. Chem. Phys.*, 6, 3423–3441, 2006.
- Wallens, S.: Modélisation des émissions des composés organiques volatils par la végétation, Ph. D. Thesis, Université Libre de Bruxelles, 2004.
- Zhang, P., B. Anderson, M. Barlow, B. Tan, and R. Myneni: Climate related vegetation characteristics derived from MODIS LAI and NDVI, *J. Geophys. Res.*, 109, D20105, doi:10.1029/2004JD004720, 2004.

Part B

Table 2. IMAGESv2 NMVOC chemistry species

Formula	Name
C ₂ H ₂	acetylene
C ₂ H ₄	ethene
C ₂ H ₆	ethane
C ₃ H ₆	propene
C ₃ H ₈	propane
C ₅ H ₈	isoprene
CH ₃ COCH ₃	acetone
CH ₃ CHO	acetaldehyde
CH ₃ OH	methanol
MEK (CH ₃ COC ₂ H ₅)	methyl ethyl ketone
(CH ₃ CO) ₂	2,3-butanedione (biacetyl)
GLY (CHOCHO)	glyoxal
CH ₃ COOH	acetic acid
CH ₃ COOOH	peracetic acid
CH ₃ CO ₃	acetyl peroxy radical
PAN (CH ₃ CO ₃ NO ₂)	peroxy acetyl nitrate
C ₂ H ₅ O ₂	ethyl peroxy radical
C ₂ H ₅ OOH	ethyl hydroperoxide
C ₂ H ₅ OH	ethanol
C ₃ H ₇ O ₂	propyl peroxy radical
C ₃ H ₇ OOH	propyl hydroperoxide
C ₂ H ₅ CHO	propanal
C ₂ H ₅ CO ₃	peroxypropionyl radical
PPN (C ₂ H ₅ CO ₃ NO ₂)	peroxypropionyl nitrate
RP (C ₂ H ₅ COOOH)	perproacid
RO ₂ (CH ₃ COCH ₂ O ₂)	peroxy radical from acetone
ROOH (CH ₃ COCH ₂ OOH)	hydroperoxide from acetone
MGLY (CH ₃ COCHO)	methylglyoxal
HYAC (CH ₂ OHCOCH ₃)	hydroxyacetone
PO ₂ (C ₃ H ₆ OHO ₂)	peroxy radical from propylene
POOH (C ₃ H ₆ OHOOH)	hydroperoxide from propylene
QO ₂ (C ₂ H ₄ OHO ₂)	peroxy radical from ethene
QOOH (C ₂ H ₄ OHOOH)	hydroperoxide from ethene
GLYALD (CH ₂ OHCHO)	glycolaldehyde
ISOPPO ₂ (C ₅ H ₈ OHO ₂)	peroxy radical from C ₅ H ₈
ISOPOOH (C ₅ H ₈ OHOOH)	hydroperoxide from C ₅ H ₈
ISON (C ₅ H ₈ OHONO ₂)	nitrates from ISOPPO ₂ +NO and C ₅ H ₈ +NO ₃
MACR (CH ₂ CCH ₃ CHO)	methylacrolein
MACRO ₂ (CHOCH ₃ CO ₂ CH ₂ OH)	peroxy radical from MACR+OH
MACROOH (CH ₃ COCHOOHCH ₂ OH)	hydroperoxide from MACR
MPAN (CH ₂ CCH ₃ CO ₃ NO ₂)	peroxymethacrylic nitrate
GCO ₃ (HOCH ₂ CO ₃)	hydroxy peroxyacetyl radical
GP (HOCH ₂ COOOH)	hydroperoxide from GCO ₃
GPAN (HOCH ₂ COOONO ₂)	peroxyacetyl nitrate from GCO ₃
KO ₂ (CH ₃ COC ₂ H ₅ OHO ₂)	peroxy radical from MEK
C ₄ H ₁₀	surrogate for the other NMVOCs

Table 3. IMAGESv2 NMVOC chemical mechanism

<i>Reaction</i>	<i>Rate</i> [Reference]
$\text{C}_2\text{H}_2 + \text{OH} \rightarrow 0.364\text{HCOOH} + 0.364\text{CO}$ +0.364HO ₂ +0.636GLY+0.636OH	$k_0 = 5.5(-30)$ $k_\infty = 8.3(-13)(\frac{300}{T})^2$ [1]
$\text{C}_2\text{H}_4 + \text{OH} \rightarrow \text{QO}_2$	$k_0 = 1.0(-28)(\frac{300}{T})^{4.5}$ $k_\infty = 8.8(-12)(\frac{300}{T})^{0.85}$ [1]
$\text{C}_2\text{H}_4 + \text{O}_3 \rightarrow 1.139\text{HCHO} + 0.63\text{CO} + 0.13\text{HO}_2$ +0.13OH+0.231HCOOH+0.139H ₂ O ₂	$1.2(-14) \exp(-2630/T)$ [1]
$\text{QO}_2 + \text{CH}_3\text{CO}_3 \rightarrow \text{CH}_3\text{O}_2 + \text{HO}_2$ +1.5HCHO+0.25GLYALD	$\frac{2.0(-12) \exp(500/T)}{(1+0.45(-6) \exp(3870/T))}$ [2] $\frac{2.0(-12) \exp(500/T)}{(1+2.2(+6) \exp(-3870/T))}$ [2]
$\text{QO}_2 + \text{CH}_3\text{CO}_3 \rightarrow \text{CH}_3\text{COOH} + \text{GLYALD}$	$\frac{2.54(-12) \exp(360/T)}{(1+8.14(-29) \exp(5528/T)[M])}$ [3] $\frac{2.54(-12) \exp(360/T)}{(1+1.23(+28) \exp(-5528/T)/[M])}$ [3]
$\text{QO}_2 + \text{NO} \rightarrow \text{HCHO} + \text{HO}_2 + \text{NO}_2$	$2.0(-13) \exp(1250/T)$ [3]
$\text{QO}_2 + \text{NO} \rightarrow \text{GLYALD} + \text{HO}_2 + \text{NO}_2$	$2.0(-13) \exp(190/T)$ [3]
$\text{QO}_2 + \text{HO}_2 \rightarrow \text{QOOH}$	$1.9(-12) \exp(190/T)$ [3]
$\text{QOOH} + \text{OH} \rightarrow \text{QO}_2$	$1.38(-11)$ [3]
$\text{QOOH} + \text{OH} \rightarrow \text{GLYALD} + \text{OH}$	$8.7(-12) \exp(-1070/T)$ [1]
$\text{C}_2\text{H}_6 + \text{OH} \rightarrow \text{C}_2\text{H}_5\text{O}_2 + \text{H}_2\text{O}$	$2.6(-12) \exp(365/T)$ [1]
$\text{C}_2\text{H}_5\text{O}_2 + \text{NO} \rightarrow \text{CH}_3\text{CHO} + \text{HO}_2 + \text{NO}_2$	$2.5(-12)$ [3]
$\text{C}_2\text{H}_5\text{O}_2 + \text{NO}_3 \rightarrow \text{CH}_3\text{CHO} + \text{HO}_2 + \text{NO}_2$	$7.5(-13) \exp(700/T)$ [1]
$\text{C}_2\text{H}_5\text{O}_2 + \text{HO}_2 \rightarrow \text{C}_2\text{H}_5\text{OOH} + \text{O}_2$	
$\text{C}_2\text{H}_5\text{O}_2 + \text{CH}_3\text{O}_2 \rightarrow 0.7\text{HCHO} + 0.8\text{CH}_3\text{CHO}$ +HO ₂ +0.3CH ₃ OH+0.2C ₂ H ₅ OH	$2.0(-13)$ [5]
$\text{C}_2\text{H}_5\text{OOH} + \text{OH} \rightarrow 0.5\text{C}_2\text{H}_5\text{O}_2 + 0.5\text{CH}_3\text{CHO} + 0.5\text{OH}$	$3.8(-12) \exp(200/T)$ [4]
$\text{C}_3\text{H}_6 + \text{OH} \rightarrow \text{PO}_2$	$k_0 = 8.0(-27)(\frac{300}{T})^{3.5}$ $k_\infty = 3.0(-11), F_c = 0.5$ [3]
$\text{C}_3\text{H}_6 + \text{O}_3 \rightarrow 0.54\text{HCHO} + 0.19\text{HO}_2 + 0.33\text{OH}$ +0.08CH ₄ +0.56CO+0.5CH ₃ CHO+0.31CH ₃ O ₂ +0.25CH ₃ COOH	$6.5(-15) \exp(-1900/T)$ [3]
$\text{PO}_2 + \text{CH}_3\text{CO}_3 \rightarrow \text{CH}_3\text{O}_2 + \text{CH}_3\text{CHO}$ +HCHO+HO ₂	$\frac{2.0(-12) \exp(500/T)}{(1+0.45(-6) \exp(3870/T))}$ [2]
$\text{PO}_2 + \text{CH}_3\text{CO}_3 \rightarrow \text{CH}_3\text{COOH}$ +0.35C ₂ H ₅ CHO+0.65HYAC	$\frac{2.0(-12) \exp(500/T)}{(1+2.2(+6) \exp(-3870/T))}$ [2]
$\text{PO}_2 + \text{CH}_3\text{O}_2 \rightarrow \text{HO}_2 + 0.5\text{CH}_3\text{CHO}$ +1.25HCHO+0.16HYAC +0.09C ₂ H ₅ CHO+0.25CH ₃ OH+0.25ROH	$5.92(-13)$ [6] $2.7(-12) \exp(350/T)$ [2]
$\text{PO}_2 + \text{NO} \rightarrow \text{CH}_3\text{CHO} + \text{HCHO} + \text{HO}_2 + \text{NO}_2$	$2.5(-12)$ [3]
$\text{PO}_2 + \text{NO}_3 \rightarrow \text{CH}_3\text{CHO} + \text{HCHO} + \text{HO}_2 + \text{NO}_2$	$7.5(-13) \exp(700/T)$ [5]
$\text{PO}_2 + \text{HO}_2 \rightarrow \text{POOH} + \text{O}_2$	$1.9(-12) \exp(190/T)$ [3]
$\text{POOH} + \text{OH} \rightarrow \text{PO}_2$	$2.44(-11)$ [3]
$\text{POOH} + \text{OH} \rightarrow \text{HYAC} + \text{OH}$	$8.7(-12) \exp(-615/T)$ [1]
$\text{C}_3\text{H}_8 + \text{OH} \rightarrow \text{C}_3\text{H}_7\text{O}_2$	$\frac{2.7(-12) \exp(350/T)}{(1+5.87 \exp(-816/T)(300/T)^{0.64})}$ [2,10] $\frac{2.7(-12) \exp(350/T)}{(1+0.17 \exp(816/T)(T/300)^{0.64})}$ [2,10]
$\text{C}_3\text{H}_7\text{O}_2 + \text{NO} \rightarrow \text{NO}_2 + \text{HO}_2 + \text{CH}_3\text{COCH}_3$	$1.513(-13) \exp(1300/T)$ [3]
$\text{C}_3\text{H}_7\text{O}_2 + \text{NO} \rightarrow \text{NO}_2 + \text{HO}_2 + \text{C}_2\text{H}_5\text{CHO}$	
$\text{C}_3\text{H}_7\text{O}_2 + \text{HO}_2 \rightarrow \text{C}_3\text{H}_7\text{OOH}$	
$\text{C}_3\text{H}_7\text{O}_2 + \text{CH}_3\text{CO}_3 \rightarrow \text{CH}_3\text{O}_2 + \text{HO}_2$ +0.74CH ₃ COCH ₃ +0.26C ₂ H ₅ CHO	$\frac{2.0(-12) \exp(500/T)}{(1+0.45(-6) \exp(3870/T))}$ [2]
$\text{C}_3\text{H}_7\text{O}_2 + \text{CH}_3\text{CO}_3 \rightarrow \text{CH}_3\text{COOH}$ +0.74CH ₃ COCH ₃ +0.26C ₂ H ₅ CHO	$\frac{2.0(-12) \exp(500/T)}{(1+2.2(+6) \exp(-3870/T))}$ [2]
$\text{C}_3\text{H}_7\text{OOH} + \text{OH} \rightarrow \text{C}_3\text{H}_7\text{O}_2$	$1.9(-12) \exp(190/T)$ [3]

Table 3. IMAGESv2 NMVOC chemical mechanism (cont'd)

<i>Reaction</i>	<i>Rate</i>	[Reference]
$\text{C}_3\text{H}_7\text{OOH} + \text{OH} \rightarrow 0.74\text{CH}_3\text{COCH}_3 + 0.26\text{C}_2\text{H}_5\text{CHO} + \text{HO}$	$1.8(-11)$ [3,8]	
$\text{C}_2\text{H}_5\text{CHO} + \text{OH} \rightarrow \text{C}_2\text{H}_5\text{CO}_3 + \text{H}_2\text{O}$	$4.9(-12) \exp(405/T)$ [1]	
$\text{C}_2\text{H}_5\text{CHO} + \text{NO}_3 \rightarrow \text{HNO}_3 + \text{C}_2\text{H}_5\text{CO}_3$	$3.46(-12) \exp(-1862/T)$ [3]	
$\text{C}_2\text{H}_5\text{CO}_3 + \text{CH}_3\text{O}_2 \rightarrow \text{HCHO} + \text{HO}_2 + \text{C}_2\text{H}_5\text{O}_2$	$1.68(-12) \exp(500/T)$ [6]	
$\text{C}_2\text{H}_5\text{CO}_3 + \text{CH}_3\text{O}_2 \rightarrow \text{RCOOH} + \text{HCHO}$	$1.87(-13) \exp(500/T)$ [6]	
$\text{C}_2\text{H}_5\text{CO}_3 + \text{CH}_3\text{CO}_3 \rightarrow \text{CH}_3\text{O}_2 + \text{C}_2\text{H}_5\text{O}_2$	$2.50(-12) \exp(500/T)$ [2]	
$\text{C}_2\text{H}_5\text{CO}_3 + \text{NO}_2 \rightarrow \text{PPN}$	$k_0 = 9.0(-28)(300/T)^{8.9}$ $k_\infty = 7.7(-12)(300/T)^{0.2}$ [1]	
$\text{PPN} \rightarrow \text{C}_2\text{H}_5\text{CO}_3 + \text{NO}_2$	$K_{eq} = 9.0(-29) \exp(14000/T)$ [1]	
$\text{C}_2\text{H}_5\text{CO}_3 + \text{NO} \rightarrow \text{NO}_2 + \text{C}_2\text{H}_5\text{O}_2$	$8.1(-12) \exp(270/T)$ [2]	
$\text{C}_2\text{H}_5\text{CO}_3 + \text{HO}_2 \rightarrow \text{RP}$	$\frac{4.3(-13) \exp(1040/T)}{(1+0.003 \exp(1430/T))}$ [2]	
$\text{C}_2\text{H}_5\text{CO}_3 + \text{HO}_2 \rightarrow \text{RCOOH} + \text{O}_3$	$\frac{4.3(-13) \exp(1040/T)}{(1+330 \exp(-1430/T))}$ [2]	
$\text{RP} + \text{OH} \rightarrow \text{C}_2\text{H}_5\text{CO}_3$	$4.42(-12)$ [3]	
$\text{RCOOH} + \text{OH} \rightarrow \text{C}_2\text{H}_5\text{O}_2 + \text{CO}_2 + \text{H}_2\text{O}$	$1.16(-12)$ [3]	
$\text{C}_5\text{H}_8 + \text{OH} \rightarrow \text{ISOPPO}_2$	$2.54(-11) \exp(410/T)$ [7]	
$\text{C}_5\text{H}_8 + \text{O}_3 \rightarrow 0.65\text{MACR} + 0.58\text{HCHO} + 0.1\text{MACRO}_2 + 0.1\text{CH}_3\text{CO}_3 + 0.08\text{CH}_3\text{O}_2 + 0.28\text{HCOOH} + 0.14\text{CO} + 0.09\text{H}_2\text{O}_2 + 0.25\text{HO}_2 + 0.25\text{OH}$	$7.86(-15) \exp(-1913/T)$ [7]	
$\text{C}_5\text{H}_8 + \text{NO}_3 \rightarrow \text{ISON}$	$3.03(-12) \exp(-446/T)$ [7]	
$\text{ISOPPO}_2 + \text{NO} \rightarrow \text{NO}_2 + \text{MACR} + \text{HCHO} + \text{HO}_2$	$2.43(-12) \exp(360/T)$ [7]	
$\text{ISOPPO}_2 + \text{NO} \rightarrow \text{ISON}$	$0.11(-12) \exp(360/T)$ [7]	
$\text{ISOPPO}_2 + \text{HO}_2 \rightarrow \text{ISOPPOOH}$	$2.05(-13) \exp(1300/T)$ [7]	
$\text{ISOPPO}_2 + \text{ISOPPO}_2 \rightarrow 2\text{MACR} + \text{HCHO} + \text{HO}_2$	$2.0(-12)$ [7]	
$\text{ISOPPOOH} + \text{OH} \rightarrow \text{MACR} + \text{OH}$	$1.0(-10)$ [7]	
$\text{ISON} + \text{OH} \rightarrow \text{MACR} + 0.5\text{CO} + 0.5\text{HO}_2 + \text{HNO}_3$	$1.5(-11)$ [3,8]	
$\text{MACR} + \text{OH} \rightarrow \text{MACRO}_2$	$2.065(-12) \exp(452/T) + 0.93(-11) \exp(175/T)$ [7]	
$\text{MACR} + \text{O}_3 \rightarrow 0.9\text{MGLY} + 0.45\text{HCOOH} + 0.32\text{HO}_2 + 0.22\text{CO} + 0.19\text{OH} + 0.1\text{CH}_3\text{CO}_3$	$0.68(-15) \exp(-2112/T) + 3.755(-16) \exp(-1521/T)$ [7]	
$\text{MACRO}_2 + \text{NO} \rightarrow \text{NO}_2 + 0.2\text{HYAC} + 0.21\text{CO} + 0.25\text{CH}_3\text{CO}_3 + 0.25\text{MGLY} + 0.61\text{HCHO} + 0.75\text{HO}_2 + 0.5\text{GLYALD} + 0.04\text{GLY}$	$2.54(-12) \exp(360/T)$ [7,8]	
$\text{MACRO}_2 + \text{HO}_2 \rightarrow \text{MACROOH}$	$1.82(-13) \exp(1300/T)$ [7]	
$\text{MACRO}_2 + \text{MACRO}_2 \rightarrow \text{HYAC} + \text{CH}_3\text{COCHO} + 0.5\text{HCHO} + 0.5\text{CO} + \text{HO}_2$	$2.0(-12)$ [7]	
$\text{MACRO}_2 + \text{NO}_2 \rightarrow \text{MPAN}$	$k_0 = 1.2(-29)(\frac{300}{T})^{5.6}$ $k_\infty = 1.1(-12)(\frac{300}{T})^{1.5}$ [8]	
$\text{MPAN} \rightarrow \text{MACRO}_2 + \text{NO}_2$	$k_0 = 9.7(-29)(300/T)^{5.6}$ $k_\infty = 9.3(-12)(300/T)^{1.5}$ $K_{eq} = 9.0(-29) \exp(14000/T)$ [7]	
$\text{MPAN} + \text{OH} \rightarrow 0.5\text{HYAC} + \text{NO}_2 + 0.5\text{CO} + \text{GLYALD}$	$3.6(-12)$ [7,8]	
$\text{MACROOH} + \text{OH} \rightarrow \text{MACRO}_2$	$2.82(-11)$ [3]	
$\text{HYAC} + \text{OH} \rightarrow \text{CH}_3\text{COCHO} + \text{HO}_2$	$2.15(-12) \exp(305/T)$ [9]	
$\text{MGLY} + \text{OH} \rightarrow \text{CH}_3\text{CO}_3 + \text{CO} + \text{H}_2\text{O}$	$8.4(-13) \exp(830/T)$ [5]	
$\text{MGLY} + \text{NO}_3 \rightarrow \text{HNO}_3 + \text{CO} + \text{CH}_3\text{CO}_3$	$3.46(-12) \exp(-1862/T)$ [3]	
$\text{CH}_3\text{COCH}_3 + \text{OH} \rightarrow \text{RO}_2 + \text{H}_2\text{O}$	$1.33(-13) + 3.82(-11) \exp(-2000/T)$ [6]	
$\text{RO}_2 + \text{NO} \rightarrow \text{NO}_2 + \text{HCHO} + \text{CH}_3\text{CO}_3$	$2.8(-12) \exp(300/T)$ [2]	
$\text{RO}_2 + \text{HO}_2 \rightarrow \text{ROOH} + \text{O}_2$	$8.6(-13) \exp(700/T)$ [2]	
$\text{RO}_2 + \text{CH}_3\text{O}_2 \rightarrow 0.3\text{CH}_3\text{CO}_3 + 0.5\text{HCHO} + 0.2\text{HO}_2 + 0.2\text{HYAC} + 0.5\text{MGLY} + 0.5\text{CH}_3\text{OH}$	$7.5(-13) \exp(500/T)$ [2,6]	

Table 3. IMAGESv2 NMVOC chemical mechanism (cont'd)

<i>Reaction</i>	<i>Rate</i>	[Reference]
ROOH+OH→RO ₂ +H ₂ O	3.8(-12) exp(200/T)	[11,3]
ROOH+OH→MGLY+OH	8.39(-12)	[3]
CH ₃ CHO+OH→CH ₃ CO ₃ +H ₂ O	4.4(-12) exp(365/T)	[10]
CH ₃ CHO+NO ₃ →CH ₃ CO ₃ +HNO ₃	1.4(-12) exp(-1860/T)	[10]
CH ₃ CO ₃ +HO ₂ →CH ₃ COOOH	$\frac{4.3(-13) \exp(1040/T)}{(1+0.003 \exp(1430/T))}$	[2]
CH ₃ CO ₃ +HO ₂ →CH ₃ COOH+O ₃	$\frac{4.3(-13) \exp(1040/T)}{(1+330 \exp(-1430/T))}$	[2]
CH ₃ CO ₃ +NO→CH ₃ O ₂ +NO ₂ +CO ₂	8.1(-12) exp(270/T)	[2]
CH ₃ CO ₃ +NO ₂ →PAN	$k_0 = 9.7(-29)(\frac{300}{T})^{5.6}$	
	$k_\infty = 9.3(-12)(\frac{300}{T})^{1.5}$	[1]
PAN→CH ₃ CO ₃ +NO ₂	$K_{eq} = 9.0(-29) \exp(14000/T)$	[1]
PAN+OH→HCHO+NO ₂	4.0(-14)	[7]
CH ₃ CO ₃ +CH ₃ O ₂ →HCHO+HO ₂ +CH ₃ O ₂	$\frac{2.0(-12) \exp(500/T)}{(1+0.45(-6) \exp(3870/T))}$	[2]
CH ₃ CO ₃ +CH ₃ O ₂ →CH ₃ COOH+HCHO	$\frac{2.0(-12) \exp(500/T)}{(1+2.2(+6) \exp(-3870/T))}$	[2]
CH ₃ CO ₃ +CH ₃ CO ₃ →2CH ₃ O ₂ +2CO ₂	2.5(-12) exp(500/T)	[2]
CH ₃ CO ₃ +NO ₃ →CH ₃ O ₂ +NO ₂	4.0(-12)	[3]
CH ₃ COOH+OH→CH ₃ CO ₃	3.7(-12)	[3]
CH ₃ COOH+OH→CH ₃ O ₂	4.2(-14) exp(855/T)	[10]
CH ₃ OH+OH→HO ₂ +HCHO	2.9(-12) exp(-345/T)	[1]
MEK+OH→KO ₂ +H ₂ O	1.3(-12) exp(-25/T)	[10]
MEK+NO ₃ →HNO ₃ +KO ₂	8.0(-16)	[6]
KO ₂ +CH ₃ CO ₃ →CH ₃ O ₂ +CH ₃ CHO+CH ₃ CO ₃	$\frac{2.0(-12) \exp(500/T)}{(1+0.45(-6) \exp(3870/T))}$	[2]
KO ₂ +CH ₃ CO ₃ →MEK+CH ₃ COOH	$\frac{2.0(-12) \exp(500/T)}{(1+2.2(+6) \exp(-3870/T))}$	[2]
KO ₂ +NO→NO ₂ +CH ₃ CHO+CH ₃ CO ₃	2.7(-12) exp(350/T)	[2]
KO ₂ +HO ₂ →CH ₃ O ₂ +CH ₃ COCHO	7.4(-13) exp(700/T)	[2]
KO ₂ +CH ₃ O ₂ →0.5CH ₃ CHO+0.5CH ₃ CO ₃		
+0.25 MEK+0.75HCHO+0.25CH ₃ OH		
+0.25ROH+0.5HO ₂	8.37(-14)	[6]
GLYALD+OH→0.8GCO ₃ +0.2GLY+0.2HO ₂	8.0(-12)	[12]
GCO ₃ +CH ₃ O ₂ →2HCHO+2HO ₂	1.68(-12) exp(500/T)	[6]
GCO ₃ +CH ₃ O ₂ →RCOOH+HCHO	1.87(-13) exp(500/T)	[6]
GCO ₃ +CH ₃ CO ₃ →CH ₃ O ₂ +HO ₂ +HCHO	2.5(-12) exp(500/T)	[2]
GCO ₃ +HO ₂ →GP	$\frac{4.3(-13) \exp(1040/T)}{(1+0.003 \exp(1430/T))}$	[2]
GCO ₃ +HO ₂ →RCOOH+O ₃	$\frac{4.3(-13) \exp(1040/T)}{(1+330 \exp(-1430/T))}$	[2]
GCO ₃ +NO→NO ₂ +HO ₂ +HCHO	6.7(-12) exp(340/T)	[6]
GCO ₃ +NO ₂ →GPAN	$k_0 = 9.0(-28)(\frac{300}{T})^{8.9}$	
	$k_\infty = 7.7(-12)(\frac{300}{T})^{0.2}$	[1]
GPAN→GCO ₃ +NO ₂	$K_{eq} = 9.0(-29) \exp(14000/T)$	[1]
GP+OH→0.5OH+0.5GCO ₃ +0.5HCHO	3.8(-12) exp(200/T)	[6]
GLY+OH→HO ₂ +1.6CO	1.14(-11)	[3]
GLY+NO ₃ →HNO ₃ +HO ₂ +1.6CO	1.44(-12) exp(-1862/T)	[3,8]
C ₄ H ₁₀ +OH→0.8ISOPPO ₂	6.0(-11) exp(-540/T)	[13]

Notes: Read 2.14(-11) as $2.14 \cdot 10^{-11}$; T: temperature (K); [M]: the air density (mol. /cm³).

Three-body reaction rates are calculated with $k = \frac{k_0[M]}{1+k_0[M]/k_\infty} F_c^{\{1+\log_{10}(k_0[M]/k_\infty)\}^2 - 1}$, $F_c = 0.6$, unless otherwise stated. Units for first-, second-, and third-order reactions are 1/sec, cm³/mol./sec and cm⁶/mol.²/sec, respectively. Rates for equilibrium reactions calculated as $k = k_f/K_{eq}$, k_f being the rate of the formation reaction and K_{eq} the equilibrium constant. References: [1], Sander et al. (2006); [2], Tyndall et al. (2001); [3], Saunders et al. (2003); [4], Müller and Brasseur (1995); [5], Horowitz et al. (2003); [6], Evans et al. (2003); [7], Pöschl et al. (2000); [8], this work; [9], Dillon et al. (2006); [10], Atkinson et al. (2004), [11], Brasseur et al. (1998); [12], Karunanandan et al. (2006); [13], Müller and Stavrakou (2005). Formic acid (HCOOH), propanol (ROH) and propacid (RCOOH) are not treated.

Table 4. Photodissociations considered in the MNVOC chemistry meachanism of IMAGESv2

<i>Reaction</i>	<i>Cross section / Quantum yield / Products (Refs.)</i>
HCHO→CO+2HO ₂	[5]/[5]/[1]
HCHO→CO+H ₂	[5]/[5]/[1]
CH ₃ COOOH→CH ₃ O ₂ +OH+CO ₂	[5]/[c]/[1]
CH ₃ OOH→HCHO+HO ₂ +OH	[5]/[c]/[1]
CH ₃ CHO→CH ₃ O ₂ +CO+HO ₂	[5]/[5]/[1]
C ₂ H ₅ CHO→C ₂ H ₅ O ₂ +HO ₂ +CO	[5]/[5]/[1]
GLYALD→HCHO+CO+2HO ₂	[5]/[5]/[1]
GLY→2CO+2HO ₂	[5]/[5]/[1]
GLY→2CO+H ₂	[5]/[5]/[1]
GLY→HCHO+CO	[5]/[5]/[1]
CH ₃ COCH ₃ →CH ₃ CO ₃ +CH ₃ O ₂	[5]/[5]/[1]
HYAC→CH ₃ CO ₃ +HCHO+HO ₂	[5]/[i]/[1]
MGLY→CH ₃ CO ₃ +CO+HO ₂	[5]/[5]/[1]
MACR→CH ₃ CO ₃ +HCHO+CO+HO ₂	[5]/[5,d]/[3]
MEK→CH ₃ CO ₃ +C ₂ H ₅ O ₂	[6]/[6]/[1]
(CH ₃ CO) ₂ →2CH ₃ CO ₃	[a]/[a]/[1]
ISON→MACR+HCHO+HO ₂ +NO ₂	[4,b]/[4,c]/[3]
QOOH→0.17GLYALD+1.66HCHO +HO ₂ +OH	[e]/[e]/[1,2]
C ₂ H ₅ OOH→CH ₃ CHO+HO ₂ +OH	[e]/[e]/[1]
POOH→CH ₃ CHO+HCHO+HO ₂ +OH	[e]/[e]/[1]
C ₃ H ₇ OOH→0.74CH ₃ COCH ₃ +0.26C ₂ H ₅ CHO+HO ₂ +OH	[e]/[e]/[1]
ISOPOOH→MACR+HCHO+HO ₂ +OH	[e]/[e]/[3]
MACROOH→OH+0.5HYAC+0.5CO +0.5MGLY+0.5HCHO+HO ₂	[e]/[e]/[3]
ROOH→CH ₃ CO ₃ +HCHO+OH	[f]/[f]/[1]
PAN→CH ₃ CO ₃ +NO ₂	[5]/[c]/[7]
PPN→C ₂ H ₅ CO ₃ +NO ₂	[g]/[g]/[g]
MPAN→MACRO ₂ +NO ₂	[g]/[g]/[g]
GPAN→GCO ₃ +NO ₂	[g]/[g]/[g]
RP→C ₂ H ₅ O ₂ +OH	[h]/[h]/[1]
GP→HCHO+OH+HO ₂	[h]/[h]/[1]

References: [1], Saunders et al. (2003); [2], this work; [3], P'oschl et al. (2000); [4], Atkinson et al. (2004); [5], Sander et al. (2006); [6], Capouet et al. (2004); [7], M'uller and Stavrakou (2005). Notes: a) J=2·J(MGLY), based on MCM; b) Assumed to photolyse as *n*-C₄H₉ONO₂; c) Quantum yield is taken equal to 1; d) Quantum yield is equal to 0.005; e) J=J(CH₃OOH); f) J=J(CH₃OOH)+J(MEK); g) J=J(PAN); h) J=J(CH₃COOOH); i) Same as for acetone.

References

- Atkinson, R., D. L. Baulch, R. A. Cox, J. N. Crowley, R. F. Hampson, R. G. Hynes, M. E. Jenkin, M. G. Rossi, and J. Troe: Evaluated Kinetic and Photochemical Data for Atmospheric Chemistry, Vol. 1 - gas phase reactions of Ox, HOx and SOx species, *Atmos. Chem. Phys.*, 4, 1461–1738, 2004, www.iupac-kinetic.ch.cam.ac.uk.
- Brasseur, G. P., D. A. Hauglustaine, S. Walters, P. J. Rasch, J.-F. M'uller, C. Granier, and X. Tie: MOZART, a global chemistry transport model for ozone and related tracers, 1. Model description, *J. Geophys. Res.*, 103, 28,265–28,289, 1998.
- Capouet, M., J. Peeters, B. Nozière, and J.-F. M'uller: Alpha-pinene oxidation by OH: Simulations of laboratory experiments, *Atmos. Chem. Phys.*, 4, 2285–2311, 2004.
- Dillon, D. J., A. Horowitz, D. H'olscher, J. N. Crowley, L. Vereecken, and J. Peeters: Reaction of HO with hydroxyacetone ($\text{HOCH}_2\text{C}(\text{O})\text{CH}_3$): rate coefficients (233–363 K) and mechanism, *Phys. Chem. Chem. Phys.*, 8, 236–246, 2006.
- Evans M. J., A. Fiore, and D. J. Jacob: The GEOS-Chem chemical mechanism version 5-07-8, Harvard University, Cambridge, MA, USA, http://homepages.see.leeds.ac.uk/~lecmje/GEOS-CHEM/geoschem_mech.pdf, 2003.
- Horowitz, L. W., S. Walters, D. L. Mauzerall, L. K. Emmons, P. J. Rasch, C. Granier, X. Tie, J.-F. Lamarque, M. G. Schultz, G. S. Tyndall, J. J. Orlando, and G. P. Brasseur: A global simulation of tropospheric ozone and related tracers: description and evaluation of MOZART, version 2, *J. Geophys. Res.*, 108, D24, 4784, doi:10.1029/2002JD002853, 2003.
- Karunanandan, R., D. H'olscher, T. J. Dillon, A. Horowitz, J. N. Crowley, L. Vereecken, and J. Peeters: Reaction of HO with glycolaldehyde HOCH_2CHO : Rate coefficients (240–362 K) and mechanism, *J. Phys. Chem. A*, 111(5), 897–908, 2007.
- Madronich, S. and S. Flocke: The role of solar radiation in atmospheric chemistry, in *Handbook of Environmental Chemistry*, edited by: Boule, P., Springer Verlag, Heidelberg, 1–26, 1998.
- M'uller, J.-F. and G. Brasseur: A three-dimensional chemical transport model of the global troposphere, *J. Geophys. Res.*, 100, 16445–16490, 1995.
- M'uller, J.-F. and T. Stavrakou: Inversion of CO and NO_x emissions using the adjoint of the IMAGES model, *Atmos. Chem. Phys.*, 5, 1157–1186, 2005.
- Pöschl, U., R. von Kuhlmann, N. Poisson, and P. J. Crutzen: Development and intercomparison of condensed isoprene oxidation mechanisms for global atmospheric modeling, *J. Atmos. Chem.*, 37, 29–52, 2000.
- Sander, S. P., B. J. Finlayson-Pitts, R. R. Friedl, D. M. Golden, R. E. Huie, H. Keller-Rudek, C. E. Kolb, M. J. Kurylo, M. J. Molina, G. K. Moortgat, L. V. Orkin, A. R. Ravishankara, and P. H. Wine: Chemical Kinetics and Photochemical data for use in atmospheric studies, Evaluation number 15, NASA Panel for data evaluation, JPL Publication 06-2, Jet Propulsion Laboratory, Pasadena, 2006.
- Saunders, S. M., M. E. Jenkin, R. G. Derwent, M. J. Pilling: Protocol for the development of the Master Chemical Mechanism, MCM v3 (Part A): tropospheric degradation of non-aromatic volatile organic compounds, *Atmos. Chem. Phys.*, 3, 161–180, 2003.
- Tyndall, G. S., R. A. Cox, C. Granier, R. Lesclaux, G. K. Moortgat, M. J. Pilling, A. R. Ravishankara, and T. J. Wallington: Atmospheric chemistry of small organic peroxy radicals, *J. Geophys. Res.*, 106, D11, 12,157–12,182, 2001.

Part C

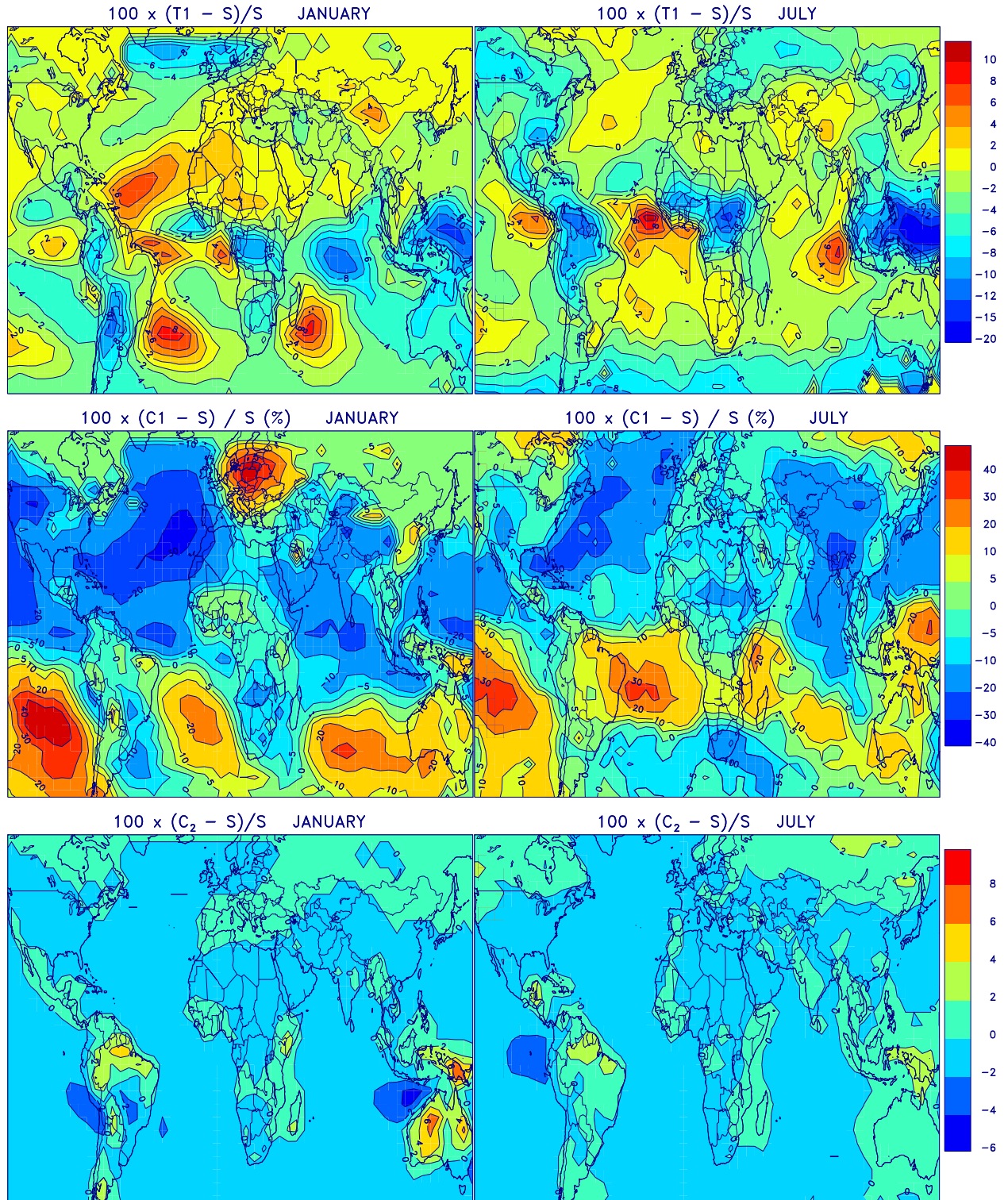


Fig. 2. Calculated change (%) in the modelled HCHO columns between the standard simulation (denoted S) and simulations using (1) doubled convective fluxes (T1, upper panel), (2) OH concentrations from Spivakovskiy et al. (1990) (C1, middle panel), and (3) isoprene degradation mechanism modified as in Lelieveld et al. (2008) (C2, lower panel).

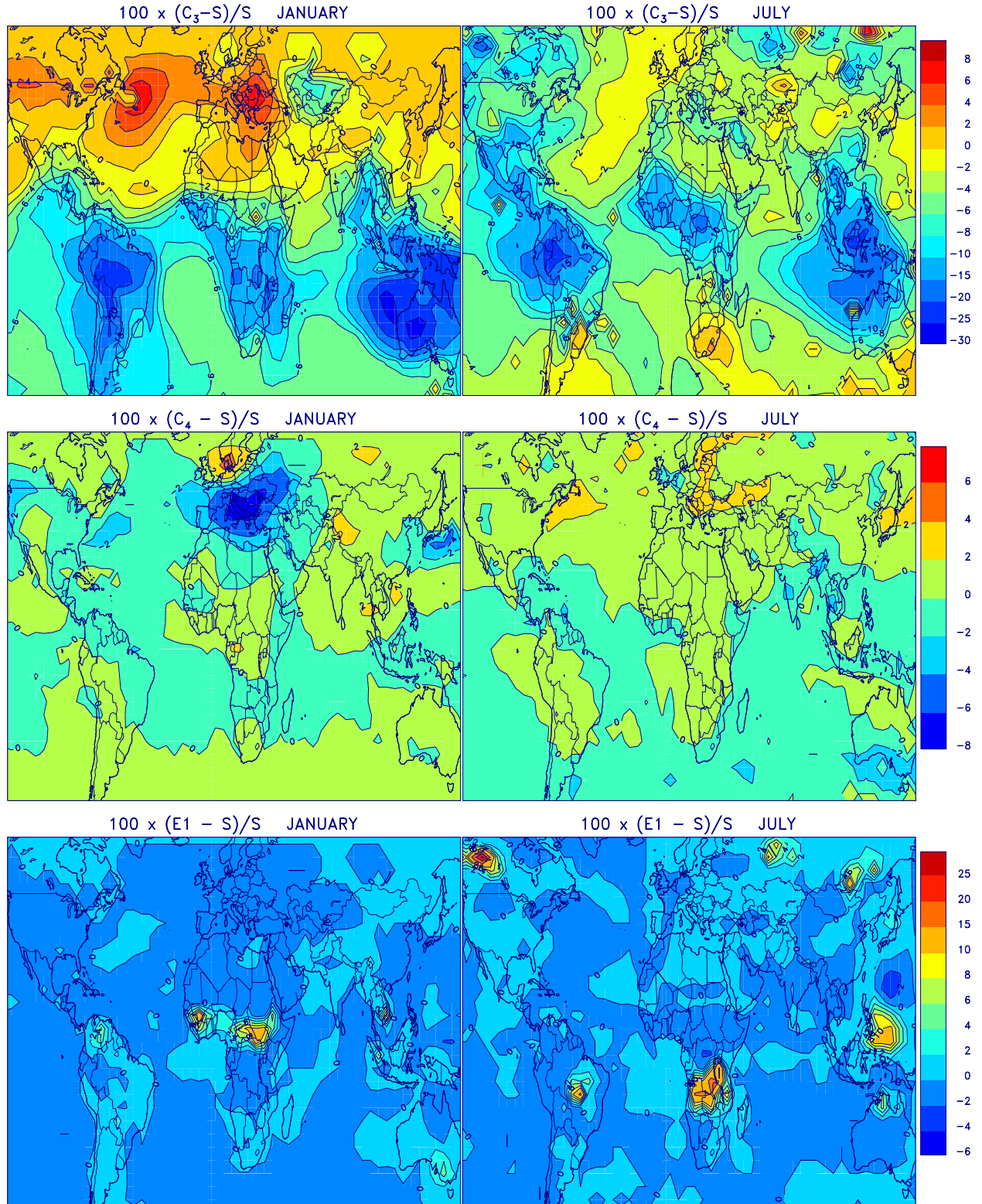


Fig. 3. As Fig.2, for simulations (1) using the isoprene degradation mechanism of the GEOS-Chem model (C_3 , upper panel), (2) with doubled cloud optical depths (C_4 , middle panel), and (3) neglecting the diurnal cycle of pyrogenic emissions (E_1 , lower panel).

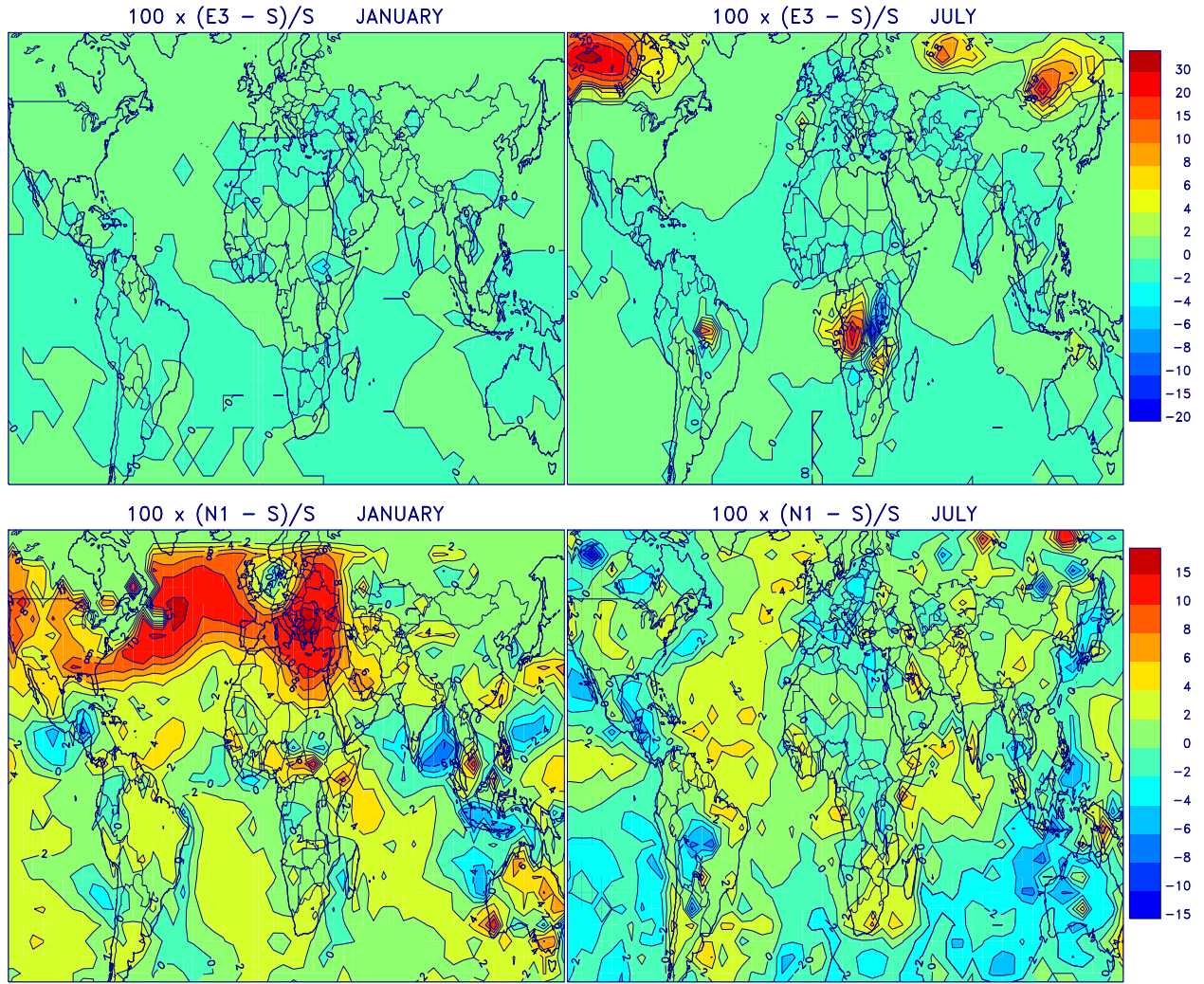


Fig. 4. As Fig.2, for simulations (1) with biomass burning emissions updated every 8 days (E3, upper panel), and (2) with an explicit calculation of the diurnal cycle throughout the entire simulation with a time step of 20 min and the KPP chemical solver (N1, lower panel).

References

- Lelieveld, J., T. M. Butler, J. N. Crowley, T. J. Dillon, H. Fischer, L. Ganzeveld, H. Harder, M. G. Lawrence, M. Martinez, D. Taraborelli, and J. Williams: Atmospheric oxidation capacity sustained by a tropical forest, *Nature*, 452, 737–740, 2008.
 Spivakovskiy, C. M., R. Yevich, J. A. Logan, S. C. Wofsy, M. B. McElroy, and M. J. Prather: Tropospheric OH in a three-dimensional chemical tracer model: An assessment based on observations of CH₃CCl₃. *J. Geophys. Res.*, 95, 18441–18471, doi:10.1029/90JD01299, 1990.